INSTITUTE OF PHYSICS PUBLISHING JOURNAL OF PHYSICS B: ATOMIC, MOLECULAR AND OPTICAL PHYSICS

J. Phys. B: At. Mol. Opt. Phys. **37** (2004) 4119–4126 PII: S0953-4075(04)80502-9

Theoretical study of the application of hollow atom production to the intensity measurement of short-pulse high-intensity x-ray sources

Kengo Moribayashi[1], **Takashi Kagawa**[2] **and Dong Eon Kim**[3]

[1] Japan Atomic Energy Research Institute, 8-1, Umemidai, Kizu-cho, Kyoto, 619-0215, Japan
[2] Department of Physics, Nara Women's University, Nara, 630-8506, Japan
[3] POSTECH, San 31, Hyoja-Dong, Namku, Pohang, Kyungbuk 790-784, Korea

E-mail: kengo@apr.jaeri.go.jp

Received 10 May 2004
Published 12 October 2004
Online at stacks.iop.org/JPhysB/37/4119
doi:10.1088/0953-4075/37/20/006

Abstract

We perform a theoretical study for the measurement of short-pulse high-intensity x-ray sources through the x-ray emission processes from multi-inner-shell excited states ($1s^2 2s^2 2p^k 3s^2 3p^2$, $k = 1$–4) and hollow atoms ($1s^2 2s^2 3s^2 3p^2$) of Si. We discuss the effect of weak-intensity long-pulse x-rays mixed with high-intensity short-pulse x-rays and the ratio of the x-ray emission from multi-inner-shell excited states with that from hollow atoms.

1. Introduction

Recent rapid progress in high intensity laser pulse technology has made possible new high-intensity short-pulse (∼fs) x-ray sources such as from Larmor radiation [1–3] or radiation damping [4] due to the high intensity laser field. These x-ray sources are useful for (1) inner-shell ionization x-ray lasers [5–10], (2) the measurement of ultra-fast processes such as those occurring in material science [11], the photoreceptors of our eyes [12] and photosynthesis [13] and (3) the production of photo-ionized plasma [14, 15]. However, it is difficult to characterize the fs pulse x-ray sources because they are mixed with weak-intensity long-pulse x-ray emission processes such as bremsstrahlung. Therefore, we concentrate on fs-pulse x-ray sources here. We should note that x-ray free electron lasers (FEL) should also produce high-intensity short-pulse x-rays [16]. The discussions here are also useful for the x-ray FEL because weak-intensity x-rays, which follow high-intensity short-pulse x-rays, continue for more than 100 fs as shown in [16].

We have demonstrated in theory that the inner-shell excited states (IES), multi-inner-shell excited states (MIES) and hollow atoms (HA) produced by high-intensity short-pulse x-rays may be useful for the measurement of the intensity of high intensity x-ray sources. In our previous paper [17], we treated only x-ray emissions from the IES of S and Fe ions. We have

shown that the shape of the x-ray spectrum could indicate to us the photon temperature. This may be useful for x-ray astrophysics [14, 15].

Moribayashi *et al* [8] have found a new characteristic for the production of IES and HA by high-intensity short-pulse x-rays. They have devised a new x-ray laser scheme using hollow atoms, which originate from inner-shell ionization x-ray lasers pumped by very high intensity x-rays. In this case, inner-shell ionization processes surpass any other atomic processes such as auto-ionization and radiation transition processes. As a result, multi-inner-shell ionizations predominate, leading to the formation of HAs. In contrast , for an ordinary x-ray source, since auto-ionization or radiation transition processes are much faster than photo-ionized processes, further inner-shell ionizations from IES seldom occur. From this characteristic, we predict that x-ray emissions from HA inform us of the x-ray intensities of high intensity x-ray sources. In this paper, we discuss their application to the measurement of short-pulse x-ray sources. We have treated soft x-rays from the photon energies of about 100–200 eV.

2. Atomic processes

We theoretically study x-ray spectra emitted from IES ($1s^2 2s^2 2p^5 3s^2 3p^2$), MIES ($1s^2 2s^2 2p^k 3s^2 3p^2$, $k = 1$–4) and HA ($1s^2 2s^2 3s^2 3p^2$) of Si produced by high-intensity short-pulse x-rays. Figures 1(a) and (b) show the atomic processes relevant to the inner-shell ionization of Si atoms and the processes of the production of multi-inner-shell-excited states and hollow atoms produced by high intensity x-rays, respectively. The initial state is the ground state of the Si atom. We consider photo-ionization (PI), radiative transition (Ar) and auto-ionization (Aa) processes. In the case of the ground state of Si atoms ($1s^2 2s^2 2p^6 3s^2 3p^2$), the following PI processes are considered:

$$\mathrm{Si}(1s^2 2s^2 2p^6 3s^2 3p^2) + h\nu \rightarrow \mathrm{Si}^+(1s^2 2s^2 2p^6 3s^2 3p) + e^-, \quad (1)$$

$$\mathrm{Si}(1s^2 2s^2 2p^6 3s^2 3p^2) + h\nu \rightarrow \mathrm{Si}^+(1s^2 2s^2 2p^6 3s 3p^2) + e^-, \quad (2)$$

$$\mathrm{Si}(1s^2 2s^2 2p^6 3s^2 3p^2) + h\nu \rightarrow \mathrm{Si}^+(1s^2 2s^2 2p^5 3s^2 3p^2) + e^-, \quad (3)$$

$$\mathrm{Si}(1s^2 2s^2 2p^6 3s^2 3p^2) + h\nu \rightarrow \mathrm{Si} + (1s^2 2s 2p^6 3s^2 3p^2) + e^-. \quad (4)$$

On the other hand, from the IES, the Ar and Aa processes are given by

$$\mathrm{Si}^+(1s^2 2s^2 2p^5 3s^2 3p^2) \rightarrow \mathrm{Si}^+(1s^2 2s^2 2p^6 3s 3p^2) + h\nu \qquad (Ar(3s - 2p)), \quad (5)$$

$$\mathrm{Si}^+(1s^2 2s^2 2p^5 3s^2 3p^2) \rightarrow \mathrm{Si}^{2+}(1s^2 2s^2 2p^6 3s^2) + e^- \qquad (Aa(3p^2)^{-1}), \quad (6)$$

$$\mathrm{Si}^+(1s^2 2s^2 2p^5 3s^2 3p^2) \rightarrow \mathrm{Si}^{2+}(1s^2 2s^2 2p^6 3s 3p) + e^- \qquad (Aa(3s3p)^{-1}), \quad (7)$$

$$\mathrm{Si}^+(1s^2 2s^2 2p^5 3s^2 3p^2) \rightarrow \mathrm{Si}^{2+}(1s^2 2s^2 2p^6 3p^2) + e^- \qquad (Aa(3s^2)^{-1}). \quad (8)$$

Here $Aa\ (3l\ 3l')^{-1}$ ($l, l' =$ s or p) means the $3l$ and $3l'$ electrons are removed through auto-ionization. We have calculated these atomic data using Cowan's code [18] where 'Hartree–Fock (HF)' and 'configuration interaction (CI)' methods are employed.

We encountered numerical difficulties in treating a large number of coupled rate equations associated with multiplet energy levels in the IES, MIES and HA of Si in obtaining x-ray spectra due to the decay from these excited states. The same type of difficulty occurred in the analysis of x-ray spectra emitted from hollow atoms produced by the collision of highly charged ions with a solid surface. In this case a step-by-step decay model, called the multistep-capture and -loss (MSCL) model, has been developed to describe the neutralization dynamics of

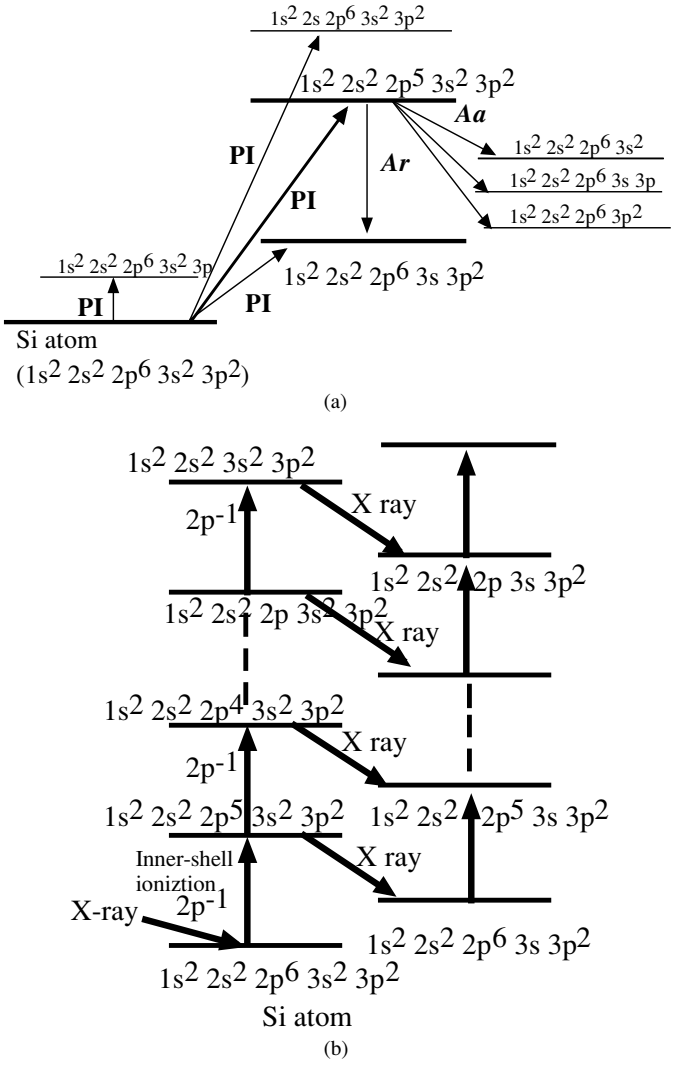

Figure 1. Atomic processes (a) together with inner-shell ionization and (b) production and x-ray emission processes of multi-inner-shell excited states and hollow atoms.

hollow atoms [19], where the multiplet structure in energy levels is approximated by using an averaging method such as the Hartree–Fock–Slater (DFS) one to reduce the number of states in the systems. In our simulation for x-ray emission from Si, we have used a model similar to the MSCL one, where configuration-averaged atomic data for energy values, transition probabilities, auto-ionization rates and photo-ionization cross sections are prepared to solve the coupled rate equations. The atomic data are averaged over the quantum numbers of spin angular momentum (S), orbital angular momentum (L) and total angular momentum (J). The averaged transition energy ($E_{\rm av}$) and the averaged atomic data of Aa and Ar are given by

$$E_{\rm av}(3{\rm s} \rightarrow 2{\rm p}) = \frac{\sum_{S,L.J} g_{SLJ} \sum_{S'L'J'} Ar_{SLJS'L'J'} E_{SLJS'L'J'}}{\sum_{S,L,J} g_{SLJ} \sum_{S'L'J'} Ar_{SLJ,S'L'J7}}, \tag{9}$$

Table 1. Atomic data for wavelengths, A_r and A_a for the Si. The values of wavelength, Ar and Aa are used in equations (9) and (10).

(M)IES	Wavelength (cm^{-1})	Photon energy (eV)	Ar (1/s)	$Aa(3p^2)^{-1}$ (1/s)	$Aa(3s3p)^{-1}$ (1/s)	$Aa(3s^2)^{-1}$ (1/s)
$2p^53s^23p^2$	7.603×10^5	94.3	0.1057×10^{11}	0.574×10^{13}	0.910×10^{13}	2.491×10^{13}
$2p^43s^23p^2$	9.224×10^5	114.6	0.3200×10^{11}	2.03×10^{13}	2.81×10^{13}	0.171×10^{13}
$2p^33s^23p^2$	1.092×10^6	135.4	0.662×10^{11}	4.51×10^{13}	5.75×10^{13}	0.525×10^{13}
$2p^23s^23p^2$	1.274×10^6	158.0	0.115×10^{12}	7.96×10^{13}	9.80×10^{13}	1.00×10^{13}
$2p\ 3s^23p^2$	1.465×10^6	181.7	0.182×10^{12}	1.25×10^{14}	1.74×10^{14}	1.78×10^{13}
$3s^23p^2$	1.667×10^6	206.7	0.265×10^{12}	1.76×10^{14}	2.04×10^{13}	2.58×10^{13}

and

$$A_{\mathrm{av}} = \frac{\sum_{S,L.J} g_{SLJ} A_{SLJ}}{\sum_{S,L,J} g_{SLJ}}, \tag{10}$$

respectively, where g_{SLJ} expresses the statistical weight of each state and the transition of $Ar_{SLJS'L'J'}$ and $E_{SLJS'L'J'}$ is $1s^22s^22p^53s^23p^{2S}L_J \rightarrow 1s^22s^22p^63s3p^{2S'}L'_{J'}$. Table 1 lists E_{av}, and the rates for Ar_{av}, and Aa_{av} processes for IES, MIES and HA of Si. For *PI*, we have calculated only the cross section ($\sigma_{PI\mathrm{Si}}$) for Si atoms. For the other ions, we use the following fitting formula for the *PI* cross sections [20]:

$$\sigma_{PI}(E_P) = \sigma_{PI\mathrm{Si}}(E_{P\mathrm{Si}}) \times \frac{B_{\mathrm{Si}}}{B} \times \frac{N}{N_{\mathrm{Si}}}, \tag{11}$$

with

$$E_{P\mathrm{Si}} = E_P \times \frac{B_{\mathrm{Si}}}{B}, \tag{11a}$$

where E_P is the photon energy and B (B_{Si}), and N (N_{Si}) are the binding energy (of Si atoms) and the number of the bound electrons (for Si atoms), respectively. The values of N_{Si} are 2, 6, 2 and 2 for the 2s, 2p, 3s and 3p electrons, respectively. We use Cowan's code [18] for the calculations of PI_{Si}. With the use of σ_{PI}, the transition rate for *PI* is given by

$$\alpha = \int \frac{I(E_P)\sigma_{PIk}(E_P)}{E_P}\,\mathrm{d}E_P, \tag{12}$$

where I is the x-ray intensity.

With these atomic rates, the population dynamics of the various atomic states as illustrated in figure 1 may be investigated by the following rate equations:

$$\begin{aligned}
\frac{\mathrm{d}P_0}{\mathrm{d}t} &= -\beta_0 P_0, \\
\frac{\mathrm{d}P_1}{\mathrm{d}t} &= \alpha_{0,1} P_0 - \beta_1 P_1, \\
&\bullet \\
&\bullet \\
&\bullet \\
\frac{\mathrm{d}P_6}{\mathrm{d}t} &= \alpha_{5,6} P_5 - \beta_6 P_6,
\end{aligned} \tag{13}$$

where P_0, P_1, P_2, ..., P_6 are the populations of the ground state, IES, MIES, ..., HA of Si, respectively, $\alpha_{m,k}$ is the transition rate via the inner-shell photo-ionization processes from the

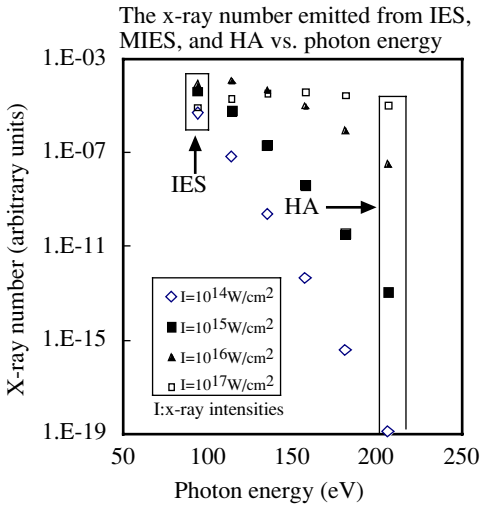

Figure 2. X-ray number (arbitrary units) emitted from IES, MIES and HA of the 2p electrons of Si ions as a function of photon energy (eV) listed in table 1 for various x-ray intensities (I) (shown by marks) assuming a 20 fs pulse of high-intensity short-pulse x-rays. The x-ray numbers from IES and HA are enclosed by rectangles.

mth to the kth state and β_k is the decay rate via Ar, Aa and PI processes in the kth state. The x-ray number (N_{hk}) is given by

$$N_{hk} = \int_0^\infty P_k Ar \, \mathrm{d}t. \tag{14}$$

3. Results and discussions

First, we should note that our model, where we have used average atomic data given in equations (9)–(11) due to too many states, can be applied for a qualitative comparison with experimental results as shown in [19] though the quantity of our calculation may not be good.

Figure 2 shows the x-ray number emitted from IES, MIES and HA of the 2p electrons of Si ions as a function of wavelength listed in table 1. The marks in the figures correspond to the x-ray intensities ($I = 10^{14}$–10^{17} W cm^{-2}) of 20 fs pulse x-ray sources. The increase of the wavelength implies that the inner-shell ionization processes take place more often, that is, the number of the inner-shell 2p electrons decreases. For less than $I = 10^{15}$ W cm^{-2}, the x-ray number of the hollow atoms is much smaller than that of inner-shell excited states. However, for more than $I = 10^{16}$ W cm^{-2}, both become almost the same. This means that it becomes easier to measure HA as the x-ray intensity increases.

We investigated the effect of weak-intensity long-pulse x-rays mixed with high-intensity short-pulse x-rays on the production of IES, MIES and HA. We consider x-rays with a pulse duration of 20 fs and an intensity of 10^{16} W cm^{-2} and for pulses of 1 ps and 10 ps and an intensity of

$$I_L = n \times I_s, \tag{15}$$

where I_S and I_L are the intensities of high-intensity short-pulse and weak-intensity long-pulse x-rays, respectively. Figure 3 shows the effect of the weak-intensity long-pulse x-rays on the

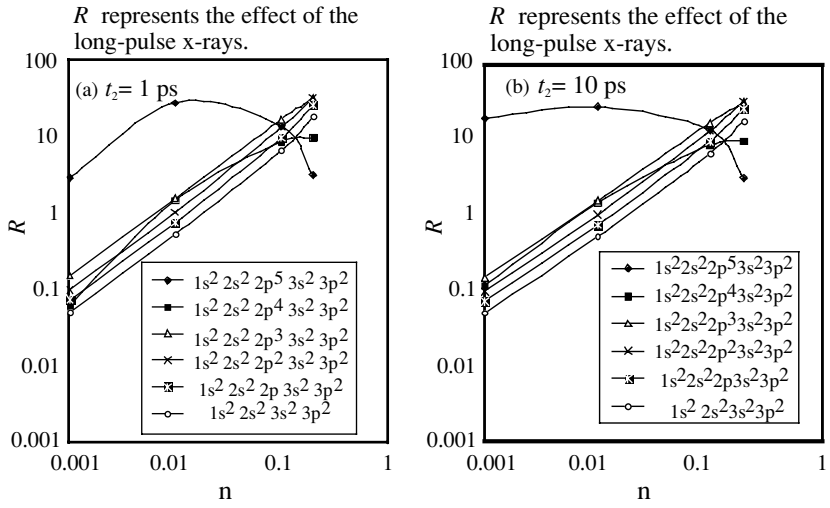

Figure 3. R versus n for IES, MIES and HA, where R and n are defined by equations (16) and (15), respectively: (a) $t_2 = 1$ ps and (b) $t_2 = 10$ ps where t_2 is the pulse length of the weak-intensity long-pulse x-rays. The values of R represent the effect of the weak-intensity long-pulse x-rays.

production of the IES, MIES and HA as a function of n ($n = 0.001$–0.1). In order to show this effect, we introduce the parameter R defined by

$$R = \frac{(Y - Y_S)}{Y_S} \times 100, \tag{16}$$

where Y and Y_S correspond to the x-ray number with and without weak-intensity long-pulse x-rays, that is, R increases in accordance with the effect of the weak-intensity long-pulse x-rays. Figures 3(a) and (b) correspond to $t_2 = 1$ ps and 10 ps, respectively, where t_2 is the pulse length of the weak-intensity long-pulse x-rays. For small n, $n \leqslant 0.01$, only the values of R for IES are larger than those for MIES and HA. Furthermore, the effect of weak-intensity long-pulse x-rays on the production of MIES and HA may be ignored because R has small values ($<1\%$) and is almost the same between $t_2 = 1$ ps (figure 3(a)) and 10 ps (figure 3(b)). Therefore, it is found that the x-rays from MIES and HA are better for the measurement of ultra-fast processes than those from IES.

Figures 4(a) and (b) show the ratio of the x-ray number from the (a) $1s^2 2s^2 2p3s^2 3p^2$ and (b) $1s^2 2s^2 2p^2 3s^2 3p^2$ with those from (a) $1s^2 2s^2 3s^2 3p^2$ and (b) $1s^2 2s^2 2p3s^2 3p^2$ as a function of pulse duration for various x-ray intensities of x-ray sources respectively. The ratio remains almost constant for pulses (>20 fs) and depends strongly on the x-ray intensities. Namely, we may use the ratio for the measurement of the x-ray intensities of high-intensity short-pulse x-ray sources.

As mentioned in section 1, fs-pulse x-ray sources are useful for the measurement of ultra-fast processes. Therefore, it is very important to measure ultra-short-pulse x-rays. Recently, Ritcher *et al* have measured short-pulse x-rays based on the photo-ionization of a rare gas [21]. On the other hand, we propose to use the characteristic of MIES and HA, that is, very fast decay and the special conditions required for their generation. We have found some advantages in the measurement of x-ray emission from MIES and HA from figures 3 and 4 as follows; (i) we may be able to remove the effect of long pulse x-rays (see figure 3), which is useful for the measurement of ultra-fast processes, (ii) we may measure the x-ray intensities

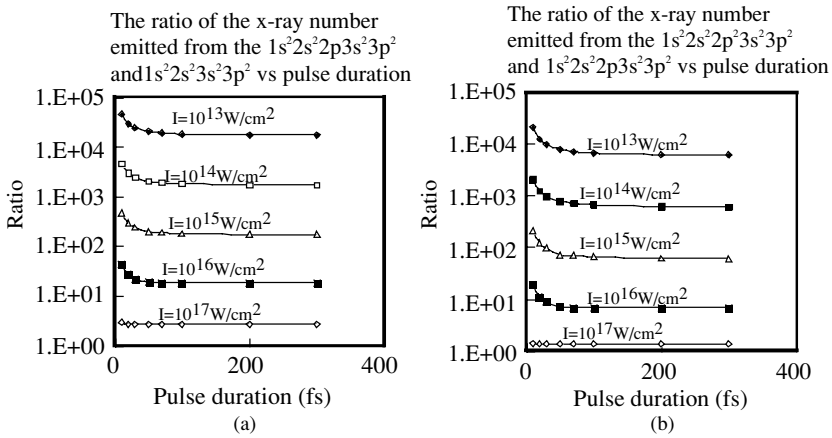

Figure 4. The ratio of the x-ray number emitted from the (a) $1s^22s^22p3s^23p^2$ ((b) $1s^22s^22p^23s^23p^2$) with those from (a) $1s^22s^23s^23p^2$ ((b) $1s^22s^22p3s^23p^2$) versus pulse duration for various x-ray source intensities (I).

of fs-pulse x-ray sources by the measurement of the ratio between the x-ray emission from MIES and HA (see figure 4).

4. Conclusions

We found that x-rays, which are emitted from MIES and HA of Si ions excited by high intensity x-ray sources, are greatly affected by high-intensity short-pulse x-rays and little by weak-intensity long-pulse x-rays. The ratio of the x-ray intensities from HA to those from the MIES becomes almost independent of the pulse length and dependent on the intensities of the x-ray sources. These ratios may be used for the measurement of intensities of high-intensity short-pulse x-ray sources.

Acknowledgments

We wish to thank Professor T Tajima and Drs J Koga and M Yamagiwa for their useful discussions and the Core University Programme between KOSEF and JSPS for support. D E Kim would like to thank the Korea Research Foundation (KRF-2000-015-DP0175) for support.

References

[1] Ueshima Y, Kishimoto Y, Sasaki A and Tajima T 1999 *Laser and Particle Beam* **17** 45
[2] Lee K, Cha Y H, Shin M S, Kim B H and Kim D 2003 *Phys. Rev.* E **67** 026502
[3] Lee K, Cha Y H, Shin M S, Kim B H and Kim D 2003 *Opt. Exp.* **11** 309
[4] Zhidkov A, Koga J, Sasaki A and Uesaka M 2002 *Phys. Rev. Lett.* **88** 185002
[5] Duguay M A and Rentzepis M 1967 *Appl. Phys. Lett.* **10** 350
[6] Kapteyn H C 1992 *Appl. Opt.* **31** 4391
[7] Moon S J, Eder D C and Strobel G L 1994 *AIP Conference Proceedings* vol 332 p 262
[8] Moribayashi K, Sasaki A and Tajima T 1998 *Phys. Rev.* A **58** 2007
[9] Moribayashi K, Sasaki A and Tajima T 1999 *Phys. Rev.* A **59** 2732
[10] Kim D, Son S H, Kim J H, Toth C and Barty C P J 2001 *Phys. Rev.* A **63** 023806

[11] Guo T, Petruck C R, Jimenez R, Ràksi F, Squier J, Walker B, Wilson K R and Barty C P J 1997 *Proc. SPIE* **3157** 84
[12] Kandori H, Sasabe H, Nakanishi K, Yoshizawa T, Mizukami T and Shichida Y 1996 *J. Am. Chem. Soc.* **118** 320
[13] Akimoto S, Takaichi S, Ogata T, Nishimura Y, Yamazaki I and Mimuro M 1996 *Chem. Phys. Lett.* **260** 147
[14] Paerels F, Cottam J, Sako M, Liedahl D A, Brinkman A C, van der Meer R L J, Kaastra J S and Predehl P 2000 *Astrophys. J.* **553** L135
[15] Liedahl D A and Paerels F 1996 *Astrophys. J.* **468** L33
[16] Ayvazyan A *et al* 2002 *Phys. Rev. Lett.* **88** 104802
[17] Moribayashi K, Kagawa T and Kim D E 2003 *Nucl. Instrum. Methods Phys. Res.* B **205** 334
[18] Cowan R D 1968 *J. Opt. Soc. Am.* **58** 808
[19] Suto K and Kagawa T 1998 *Phys. Rev.* A **58** 5004
Suto K and Kagawa T 2001 *Phys. Rev.* A **63** 019903(E)
[20] Zel'dovich Y B and Raizer Y P 1966 *Physics of Shock Waves and High Temperature Hydrodynamics Phenomena* (New York: Academic) p 265
[21] Richter M *et al* 2003 *Appl. Phys. Lett.* **83** 2970